HHS Public Access

Author manuscript

Int J Pharm. Author manuscript; available in PMC 2016 May 15.

Published in final edited form as:

Int J Pharm. 2015 May 15; 485(0): 7–14. doi:10.1016/j.ijpharm.2015.02.059.

Synthesis and Characterization of Silk Fibroin Microparticles for Intra-Articular Drug Delivery

Timothy K. Mwangi, B.S.[1], **Robby D. Bowles, Ph.D**[1], **David M. Tainter, B.S.**[2], **Richard D. Bell, B.S.**[2], **David L. Kaplan, Ph.D**[3,*], and **Lori A. Setton, Ph.D**[1,2]

[1]Dept of Biomedical Engineering, Duke University, Durham, NC

[2]Department of Orthopaedic Surgery, Duke University Medical Center, Durham, NC

[3]Dept of Biomedical Engineering, Tufts University, Medford, MA

Abstract

Objective—To determine the utility of silk fibroin (SF) microparticles as sustained release vehicles for intra-articular delivery.

Design—SF formulations were varied to generate microparticle drug carriers that were characterized *in vitro* for their physical properties, release kinetics for a conjugated fluorophore (Cy7), and *in vivo* for intra-articular retention time using live-animal, fluorescence *in vivo* imaging.

Results—SF microparticle carriers were spherical in shape and ranged from 598 nm to 21.5 μm in diameter. SF microparticles provided for sustained release of Cy7 *in vitro*, with only 10% of the initial load released over 7 days. Upon intra-articular injection in rat knee joints, the SF microparticles were associated with an intra-articular fluorescence decay half-life of 43.3 hours, greatly increasing the joint residence over that for an equivalent concentration of SF-Cy7 in

*Corresponding Address: Lori A. Setton, Department of Biomedical Engineering, 136 Hudson Hall, Box 90281, Durham, NC 27708, Phone: 919-660-5131, Fax: 919-681-4890, lori.setton@duke.edu.

Competing Interests

There are no competing interests or conflicts of interest to report.
Authors have no conflicts of interest.

Author Contributions

TKM made significant contributions to the design, execution, and analysis of this work. TKM led the experiments and was in charge of analyzing the data. TKM drafted the manuscript and contributed to the revision of the manuscript to ready it for submission. RobbyDB provided significant contribution in the design and implementation of the experiment. RobbyDB helped to acquire the necessary imaging data for the work and contributed to the revision of the manuscript. DMT provided substantial support in the execution of the work by performing the animal injections and assisted in the collection of the imaging data. Richard DB provided substantial contribution to the analysis of the imaging data by writing the source code for the analysis of the imaging data. DLK provided substantial contributions to the design of the work and provided the native silk cocoons as a starting material for the work. DLK also contributed substantially to the revision of the manuscript. LAS is the lead investigator of this work, and provided a substantial contribution to the design, analysis, and interpretation of the work. LAS also contributed heavily to the revision of the manuscript. All authors have read and approved the final manuscript, and each author contributed to the revising of the final manuscript. All authors are accountable for all aspects of the work, ensuring all elements pertaining to accuracy and integrity have been addressed.

solution form. The SF microparticles also increase the localization of dye within the joint cavity as determined by image analysis of fluorescent gradients, significantly reducing distribution of the Cy7 to neighboring tissue as compared to SF-Cy7 in free solution.

Conclusion—Silk microparticles act to provide for localized and sustained delivery of loaded small molecules following intra-articular injection, and may be an attractive strategy for delivering small molecule drugs for the treatment of arthritis.

Keywords

intra-articular; drug delivery; silk fibroin; microparticles; *in vivo* imaging; osteoarthritis

Introduction

Osteoarthritis (OA) is a degenerative disease of articular joints that impacts nearly 27 million Americans or 12.1% of US adults (Bitton 2009). The disease is characterized by progressive deterioration of the cartilage lining, subchondral bone destruction and thickening of the joint capsule (Gerwin et al. 2006, Hough Jr. 2005, Poole and Howell 2001). These tissue changes lead to symptomatic joint pain and joint dysfunction, leading to restrictions on daily life activities. The first and most widely prescribed pharmacological treatment for osteoarthritis is the oral administration of non-steroidal anti-inflammatory drugs (NSAIDs) to reduce inflammation and treat symptomatic pain. While NSAIDs have been shown to have an effect on pain management, the long term use of systemic NSAIDs does not modify OA progression and has been associated with side-effects. When NSAID therapy provides no benefit, intra-articular injection of corticosteroids or hyaluronan may be prescribed (Zhang et al. 2008). While corticosteriods and other disease-modifying drugs may have benefits when administered to the affected joint, their benefits are limited by the rapid clearance of small-molecule drugs from the knee joint (Evans et al. 2014, Gerwin et al. 2006, Wallis et al. 1985). The benefits of glucocorticoid injections are often short-lived (1–4 weeks), necessitating frequent injections to maintain efficacy (Ayral 2001, Jones and Doherty 2003). Small-molecule drugs, such as methotrexate and diclofenac, may also have therapeutic potential for treatment of arthritis, but have also been shown to have intra-articular half-lives as short as one to two hours following intra-articular injection (Owen et al. 1994, Wigginton et al. 1980).

In order to increase the residence time of small-molecule drugs that may have efficacy in treating arthritis, a broad set of drug delivery strategies have been developed that can allow for the slow and sustained release of drug into the articular cavity (Kang and Im 2014). These strategies include encapsulation of drug in natural materials, such as chitosan, alginate, albumin protein, and elastin-like polypeptides, as well as synthetic materials such as polymers and lipids. Polymeric, drug-loaded particles, such as those constructed from materials such as poly-(lactide-co-glycolide) acid (PLGA) have been most widely studied for the delivery of small molecules to the joint space, and are now the subject of a clinical trial for the delivery of triamcinolone (Butoescu et al. 2009, Horisawa et al. 2002, Kumar 2013, Liang et al. 2004). Similarly, liposomes have been developed to release dexamethasone following delivery to the joint space (Butoescu et al. 2009, Lopez-Garcia et al. 1993, Turker et al. 2005). These clinical studies demonstrate that synthetic microparticles

have utility in releasing drug following intra-articular delivery, yet to date no polymeric drug delivery system has been approved for intra-articular administration in humans (Butoescu et al. 2009, Gerwin et al. 2006). While polymeric and lipid carriers have been most widely proposed, naturally-derived delivery vehicles may provide the benefit of biocompatibility and low cost. One of the earliest demonstrations of a biologically-based drug carrier systems for intra-articular injection were albumin microparticles, formed by emulsion and cross-linking, for the delivery of rose bengal (Ratcliffe et al. 1987). *In vitro* release studies showed that drug was poorly retained within the microparticles during incubation in serum, which was further confirmed by *in vivo* studies that revealed little difference in joint concentration between free drug injection and drug-loaded particles after 24 hours. Elastin-like polypeptides (ELPs), recombinant proteins based on a native elastin sequence that can transition into drug depots *in situ*, provide another example of a pseudo-naturally derived delivery vehicle that has utility in increasing protein drug residence times in the joint space (Adams et al. 2009, Allen and Cott 2010, Betre et al. 2006).

Silk fibers from the mulberry silkworm, *Bombyx mori*, have a long history of clinical use as a biomaterial, particularly as sutures and more recently as new FDA-approved medical devices. Silk fibroin, the de-gummed fibers of native silk, are a natural protein material that has proven to be non-immunogenic and robust against hydrolytic degradation (Meinel and Kaplan 2012). The protein is very hydrophobic, readily forming β-sheet secondary structures resulting in a high density of crystalline regions. These regions are nearly impenetrable to water and yield desirable degradation properties *in vivo* (Cao and Wang 2009, Numata and Kaplan 2010, Vepari and Kaplan 2007). Silk fibroin can be used to fabricate microparticles to entrap and release drug by emulsification (Wang et al. 2010). Using this method, silk microparticles (~1–20μm) can be easily and reproducibly formed with high loading efficiencies for small-molecule drugs and slow release rates (5–50% in first 168 hours). In this study, we explored the utility of silk fibroin microparticles developed for intra-articular drug delivery of small-molecule drugs by adapting the method for silk microparticle fabrication to incorporate conjugation of a fluorescent dye. *In vitro* studies of fluorophore release and measures of the intra-articular clearance of fluorophore from rat knee joints using live-animal, fluorescence *in vivo* imaging (Bowles et al. 2013, Whitmire et al. 2012), were performed to assess the potential for the silk microparticles to contribute to sustained release in this application.

Materials and Methods

Study Design

In order to assess the utility of silk fibroin (SF) microparticles for intra-articular drug delivery of small molecules, particles were characterized for physical properties, *in vitro* release kinetics, and *in vivo* intra-articular retention in rat knee joints. The physical properties of particle size, dispersity and surface morphology were assessed by scanning electron microscopy (SEM) imaging. The *in vitro* release of a model tracer, Cy7 near-infrared dye, was used to assess the effects of different formulation methods on microparticle size and release rates of bound tracer. We chose to study release of a model compound to represent potential release profiles for a range of drugs, and to enable our

detecting the release kinetics *in vivo*. Microparticles were injected into the knee joints of rats to study the *in vivo* retention of tracer within the intra-articular cavity by fluorescence *in vivo* imaging.

Silk Processing and Dye Incorporation

Methods were adapted from those presented by Rockwood and colleagues (Rockwood et al. 2011). Briefly, 5 g of pre-boiled silk cocoons were cut into small pieces and boiled for 30 min in a solution of sodium carbonate (2.12 mg/mL, Sigma-Aldrich, St. Louis, MO). The resulting silk fibroin (SF) mesh was washed in fresh distilled water (three times, 30 min each), dried overnight, and then dissolved in lithium bromide (Sigma-Aldrich, 9.3 M at 60°C for 3 h). The dissolved SF solution was dialyzed against distilled water for 72 h with several water exchanges and centrifuged at 20,000 G and 4°C for 15 min (Beckman J2-MI; Beckman Coulter, Brea, CA). The resulting 7.5–8.0% SF solution was stored immediately at 4°C until tracer dye conjugation. To conjugate Cy7 dye (Lumiprobe, Hallandale Beach, FL) to silk protein, 5 mL of SF solution was dialyzed against 0.1 M sodium bicarbonate (pH=8.3–8.5) and allowed to equilibrate. The resulting solution was then added to 100 μL of Cy7 dye (1.7 mM in methanol) and mixed slowly for 2 h to couple Cy7 molecules to primary amines on the SF protein. The product was then dialyzed overnight in 4 L of distilled water to remove unreacted fluorophore. The resulting SF-Cy7 solution was characterized by fluorescence (Enspire, Perkin Elmer; ex/em. 754/778 nm) to determine the molar ratio of bound Cy7 dye to silk protein.

Particle Fabrication

Particles were formulated from SF-Cy7 solution using an emulsion method described previously (Wang et al. 2010). The Cy7 dye was anticipated to modify the silk particle formation such that a series of optimization studies were performed to identify a repeatable particle formulation method. Cy7-labeled and unlabeled SF solutions were combined to form the following mixtures: a) SF-Cy7 protein only (**SF-Cy7$_{100\%}$**); b) SF-Cy7 mixed with unlabeled SF protein at 1:1 molar ratio (**SF-Cy7$_{50\%}$**); and c) SF-Cy7 protein mixed with unlabeled SF protein at 1:2 molar ratio (**SF-Cy7$_{33\%}$**). The SF protein mixtures were stirred in poly-vinyl alcohol (PVA) (5%) at a 1:4 (SF: PVA) mass ratio, and placed in a glass petri dishes inside a chemical fume hood to dry overnight. The dried films were re-suspended in distilled water and agitated (Rocker 35, 10 min; Labnet International Inc., Edison, NJ) to ensure complete re-suspension of silk particles. Particles were then separated from solution (20,000 G, 4°C, 15 min) and immersed in 70% methanol (MeOH), to further dehydrate the particles and increase β-sheet content for enhanced dye retention (Hofmann et al. 2006). An additional SF coating of microparticles was used in one group to test for the potential of an SF coating to limit burst release properties of Cy7 in the lowest Cy7 concentration microparticle (Gobin et al. 2006). Formed SF-Cy7$_{33\%}$ particles were immersed in 1% SF solution and shaken for 30 min, then exposed to 70% MeOH for 60 sec before centrifugation (**SF-Cy7$_{33\%}$ Coated**).

Scanning Electron Microscopy

Physical properties of each SF-Cy7 particle formulation were assessed by scanning electron microscopy (SEM). Aliquots of each particle formulation were freeze dried, and mounted on studs with gold sputter coating under vacuum pressure on a Desk IV Vacuum Sputter system (Denton, Moorestown, NJ). Particles were then imaged (FEI XL30, 12 kV, 3500 x, Philips, Amersterdam, The Netherlands) and assessed for surface morphology by visual inspection, while particle size and particle dispersity were quantified by image analysis (ImageJ®, NIH, Bethesda, MD).

In Vitro Release Study

To quantify the retention of Cy7, the different particle formulations were incubated in enzymatic release buffer (300 μL PBS with Protease XIV, 1 mg/mL) to evaluate the kinetics of Cy7 release over time under enzymatic conditions. Protease XIV has been used in release studies of SF previously at concentrations of 1–3 mg/mL, promoting biodegradation and simulating *in vivo* conditions otherwise not observed in PBS alone (Altman et al. 2003, Arai 2004, Horan et al. 2005, Kim et al. 2005, Lu et al. 2011). Particles were suspended in release buffer in microcentrifuge tubes under gentle agitation (37°C), and aliquots (200 μL) of supernatant were collected at intervals for 168 h (2, 8, 24, 48, 96, and 168 h post-incubation) by centrifugation (20,000 G, 4°C, 10 min). Aliquots were mixed with acetonitrile (1:1 volume ratio) for the measure of the concentration of released Cy7 via fluorescence (ex/em: 750/800 nm, IVIS Kinetic, Perkin Elmer, Waltham, MA). The resulting measurements are reported as cumulative percentage of the loaded Cy7 over time.

In Vivo Intra-articular Retention Study

To assess the *in vivo* intra-articular retention of the Cy7-labeled SF microparticles, live-animal, fluorescence *in vivo* imaging was used. All procedures were performed in accordance with Duke University IACUC regulations. Eight 7–8 week old, male Sprague Dawley rats (Charles River Laboratories, Wilmington, MA) were anesthetized by isoflurane and trimmed of fur on their lower limbs. Under anesthesia, fluorescence images were collected on the IVIS Kinetic *in vivo* imaging system prior to intra-articular injection (ex/em: 750 nm/800 nm). Immediately after pre-operative imaging, the rats received a 30 μL intra-articular injection in the right hind limb (Model 705 RN, Hamilton Company, Reno, NV) of a SF-$Cy7_{33\%}$ microparticle suspension (in sterile PBS) or an equivalent dye concentration in SF-Cy7 solution as a control (100 μM) under isoflurane anesthesia (n=4 per group). To ensure sterility, SF microparticles were treated with 70% ethanol for 1 min with pipette mixing, prior to centrifugation and resuspension in sterile PBS. SF-Cy7 solution was sterilized by sterile filtration (0.22 μm filter, Millipore). Longitudinal images of the animal hind limbs were taken immediately following injection and up to 120 h after injection. To analyze the intensity of fluorescence emitted from the knee joint of each animal, a circular region of interest (ROI) was selected in the area of the knee comprising the intra-articular space and centered on the location of peak fluorescence in each image; the ROI was held constant in shape and size across all images and time points (Bowles et al. 2013).The total fluorescence within the ROI for each animal at each time point was normalized to the total fluorescence measured at 2 h after injection, as this was the time of peak intra-articular

fluorescence (total normalized fluorescence, T_{NF}). T_{NF} served as a surrogate measure of Cy7 remaining inside the joint space, and was numerically fit to a mono-exponential decay equation ($y = C_0 * e^{-kt}$: $y = T_{NF}$; $C_0 = T_{NF}$ (t= 2 h); k=decay rate constant; t=time in hours). A mono-exponential decay fit was selected with normalization by the T_{NF} at the peak of 2 h to model the consistent decay in fluorescence across animals after a 2 h distribution period. The decay rate constant from each fit was used to determine a decay half-life ($t_{1/2}$) and half-lives were tested for statistical differences between groups ($t_{1/2} = \ln(2)/k$, where k = decay rate constant).

Images were further processed to infer the pattern of radial distribution of fluorescence within the joint for each group. Peak fluorescent signals in each ROI were identified and all data within each ROI were normalized by this value. Mean normalized fluorescence values were graphed as a function of radial distance from the peak for images taken immediately following injection (Time 0) and at 24 h post-injection. A mono-exponential decay curve was fit to the distribution data for each injection group to determine the radial distance at which the normalized fluorescence falls to 50% of maximum fluorescence (RD_{50}). The RD_{50} for each injection group was compared for statistical differences at times 0 and 24 h post-injection.

Statistics

All comparisons of total dye released *in vitro* from different SF-Cy7 microparticle formulations were performed by two-way analysis of variance (ANOVA) for time and formulation, with a Tukey's post-hoc test for significance at $p<0.05$. Comparisons of variables determined by mono-exponential decay curve fitting for the joint clearance of Cy7 and radial distribution (decay half-life and $RD_{50,}$ respectively) were performed by an unpaired t-test (JMP 10 software, JMP, Cary, NC).

Results

Particle Characterization

Cy7 dye was conjugated to SF at a molar ratio of 0.35:1 (Cy7: SF), forming Cy7-bound (SF-Cy7) solution for particle fabrication alone or in combination with unmodified SF solution. Cy7-labeling of silk protein impacts the formation of SF microparticles by emulsification, such that different formulations of SF-Cy7 and SF solution were investigated to identify a formulation with maximal Cy7 retention. Resulting SF-Cy7 microparticles of all formulations were found to be mainly spherical in shape with a rough, wrinkled surface morphology (Figure 1). The emulsification process yielded poly-disperse particle populations with diameters that varied from several hundred nanometers to tens of microns, depending on the particular formulation (Table 1). For this reason, the SEM method for particle size characterization was chosen over scattering methods that are accurate in a narrow range of sizes. Particles formed with SF-Cy7 solution only were largest in diameter on average and yielded the broadest range of particle sizes. Particles formed by mixing SF-Cy7 protein with unconjugated silk protein were smaller in diameter on average, and were less polydisperse.

The effects of an additional step to coat SF-Cy7 microparticles with unmodified SF was also examined in part due to prior work which showed that SF coating could significantly reduce the burst release of encapsulated drugs in liposomes. This strategy employs hydrophobic interactions between the SF domains and the lipids (Gobin et al. 2006). Added processing of SF-$Cy7_{33\%}$ particles in SF solution (1%) resulted in a mesh coating that appeared to aggregate particles together, limiting visualization of distinct spherical particles (Figure 1c). Surface morphology of coated microparticles was otherwise unaltered from the other uncoated particle formulations, but particle size often could not be determined.

In Vitro Drug Release Study

When incubated in a proteolytic solution, SF-Cy7 particles gave rise to slow and sustained release of Cy7 for all formulations (Figure 2). The greatest cumulative release of Cy7 was observed for particles formed from SF-$Cy7_{100\%}$, exhibiting a more pronounced release within the first 8h of incubation (2.2% of loaded Cy7). The kinetics of Cy7 release were slower for microparticles formed with a mixture of modified and unmodified SF, with the SF-$Cy7_{33\%}$ particles releasing almost a third of that released by the SF-$Cy7_{100\%}$ particles at 8 h (0.85% and 2.2% of loaded Cy7, respectively; $p<0.05$). There was evidence that this observation is a function of the fraction of unmodified SF used, as significant differences in total cumulative release were observed at day 7 between SF-$Cy7_{33\%}$, SF-$Cy7_{50\%}$ and SF-$Cy7_{100\%}$ formulations (3.6%, 6.6%, and 8.2%, respectively; $p<0.05$). The effects of added SF coating as compared to the uncoated SF-$Cy7_{33\%}$ formulation upon release rates were negligible. The SF-$Cy7_{33\%}$ silk microparticles, coated and non-coated, yielded the least total cumulative release of Cy7 dye over the entire 7 d incubation period (3.1% and 3.6%, respectively; $p<0.05$ vs. SF-$Cy7_{50\%}$ and SF-$Cy7_{100\%}$ microparticles). Decreasing the fraction of SF-Cy7 in formed particles, by adding unmodified SF solution to the emulsion, appears to have the greatest effect on particle stability, resulting in particles that are smaller and slower to release bound dye.

In Vivo Drug Retention Study

Intra-articular retention of Cy7 for SF-$Cy7_{33\%}$coated microparticles was measured by live-animal fluorescent imaging of rat knee joints and compared to values for a SF-Cy7 solution. In both treatment groups, total normalized fluorescence (T_{NF}) peaked in the joint between time 0 and 2h post-injection and then gradually decayed throughout the duration of the study (Figure 3). The T_{NF} measured in animals injected with SF-Cy7 protein solution decreased more rapidly than that measured in microparticle-injected limbs, as evidenced by the exponential decay half-lives for each injection group (12.6± 2.2 h and 43.3± 14.4 h respectively; $p<0.05$) (Figure 4). This suggests that the microparticles result in a greater persistence of the Cy7 dye to the joint cavity.

Fluorescence *in vivo* imaging and ROI analysis revealed differences in Cy7 fluorophore joint radial distribution between the two injection groups. At Time 0, the normalized fluorescence of SF-Cy7 microparticle-injected limbs falls rapidly away from the central peak while fluorescence for SF-Cy7 solution injected limbs falls gradually (RD_{50} = 0.17 mm and RD_{50} = 0.56 mm, respectively; $p<0.05$) (Figure 5a). This phenomena was even more pronounced after 24 h, when SF-Cy7 solution-injected joints maintained even higher

fluorescence values further away from the peak, while values still decreased steeply for microparticle-injected joints (RD_{50} = 1.0 mm and RD_{50} = 0.20 mm, respectively; $p<0.05$) (Figure 5b). This finding suggests that the Cy7 was localized to the synovial fluid and immediate synovium and joint tissue for microparticles, but was more broadly distributed when injected as a fully mobile SF-Cy7 molecule. *Ex vivo* images of the exposed joint space also qualitatively support the observation of differential distribution between groups (Figure 6). Greater peak values and more focused distribution of fluorescence is observed inside the joint capsule when joints are injected with SF-Cy7 microparticles than with SF-Cy7 solution.

Discussion

Particle Size Characterization

Drug carrier size is an important consideration for intra-articular drug delivery, that to date has not been fully resolved. Early work by Horisawa and co-workers examined the effect of particle size through the use of *poly* lactic-co-glycolic acid (PLGA) microparticles and nanoparticles. They determined that fluorescein-loaded nanoparticles (~265 nm in diameter) were readily phagocytosed and thus caused a very minimal immunogenic response from local tissue. However, microparticles (~26 μm average diameter, but ranging from 3.1–59.9 μm) were poorly phagocytosed resulting in the formation of large granulation tissue by multinucleated giant cells (Horisawa et al. 2002). Conversely, Liggins and colleagues found nearly the opposite to be true. They determined that PLGA particles of 35–105 μm in diameter were less inflammatory, producing less swelling and cell infiltration 7 days after injection, while particles of 1–20μmin size produced greater inflammation, with a great proliferation of macrophages, lymphocytes and plasma cells in the synovial membrane (Liggins et al. 2004). Still another study by Butoescu and co-workers, utilizing magnetic particles from 4–14μm in diameter, determined that microparticles on this order were safe and non-inflammatory to joint tissue up to 3 months following injection (Butoescu et al. 2009). In a later review of the field, Butoescu and co-workers would suggest that particles of 5–10 μm in diameter are the most suitable size for intra-articular drug delivery, as it ensures phagocytic uptake and prolonged drug residence time (Butoescu et al. 2009). This summary illustrates the additional work that needs to be done to understand the interaction of material constituents and particle size in contributing to an inflammatory response, as well as sustained release, in the intra-articular space. In our example working with silk fibroin microparticles here, we found that micron-sized particles of 1–20 μm dimensions did contribute to sustained residence time in the joint space, although additional work would be needed to determine the fate of the microparticles and their contribution to a potential inflammatory response.

In this study, silk fibroin microparticles of 1–21.6 μm in diameter were fabricated as carriers for a small-molecule drug for intra-articular drug delivery. These dimensions are consistent with those reported by Wang and co-workers who first formed silk microparticles by PVA emulsion (1–30 μm) (Wang et al. 2010). The size and dispersity of the protein particles varied with the composition of the particle. Particles formed with a greater fraction of unmodified silk protein resulted in smaller and less polydisperse particles. This observation

is best explained with the model of self-assembled silk microparticles presented by Lammel and co-workers (Lammel et al. 2010). The model revealed that lower pH values produced more tightly packed particles due to reduced steric hindrance between hydrophobic β-sheets. For our silk particles, steric hindrance may be a result of interactions between bound Cy7, a hydrophobic molecule, and the hydrophobic silk domains (Lammel et al. 2010). The presence of Cy7 may disrupt the packing of β–sheets within the forming microparticles leading to a less dense and more polydisperse particle population. By incorporating higher fractions of unmodified silk protein, smaller, more mono-disperse particle populations were fabricated, allowing for the study of particles over a more narrow size range. Further analysis is necessary to confirm that particles in this range do not elicit the formation of granulation tissue.

In Vitro Release Study

SF microparticles fabricated with unmodified SF yielded slower proteolytic release rates than particles fabricated from Cy7-bound silk protein only, and demonstrated a significantly reduced total release *in vitro*. These observations suggest that the unmodified SF supplementing the conjugated SF-Cy7 facilitates increased hydrophobic interactions leading to more densely-packed particles and thus slower release rates. Conversely, we saw a minimal benefit to Cy7 retention by the inclusion of a SF coating; however, SEM analysis revealed that this processing step results in networking or aggregation of microparticles. This was seen as a favorable quality for joint retention following injection, as ultrafiltration through the synovial membrane is the source of rapid joint clearance of injected solutes. Therefore, coated SF-$Cy7_{33\%}$ microparticles were utilized for subsequent *in vivo* intra-articular injection studies.

In our study, the total bound dye released from SF-Cy7 conjugate microparticles never exceeded 10% of loaded Cy7 over the 160 h period during which release was measured. This finding is consistent with the release of hydrophobic small molecules from other formed SF materials. Wang and co-workers determined that approximately 5% of loaded Rhodamine B, a hydrophobic small-molecule, was released over 14 d under similar enzymatic conditions (Wang et al. 2010). Similarly, Lammel and co-workers determined that hydrophobic and neutral small-molecules, passively encapsulated in silk microparticles, were released at a rate of only 20–25% or 35–40%, respectively, over the first 7 days (Lammel et al. 2010). Although these values were greater than that observed in our study, our small-molecule was covalently bound to the silk protein potentially contributing to the reduced release. The slow and sustained release of these model drugs in all studied systems suggests a protracted degradation of silk biomaterials due to a slow, long-term degradation of the crystalline regions of the SF (Arai 2004, Cao and Wang 2009, Horan et al. 2005, Meinel et al. 2005, Srihanam et al. 2009). This makes SF an excellent material for slow, sustained release of loaded small-molecule drugs.

In Vivo Intra-articular Retention Study

Live-animal, fluorescence imaging is a useful tool to examine an ability for drug carrier technologies to improve drug residence times within the joint space. Fluorophore scattering greatly limits an ability to accurately measure localization to the injected compartment,

however as compared to radioisotope scintigraphy. In this experiment, we chose to compare injections of dye-bound SF microparticle suspensions to a dye-bound SF protein in solution. We sought to assess the relative magnitude and radial distribution of injected dye by live-animal fluorescence imaging for comparison of both joint distribution and joint clearance characteristics.

All fluorescence intensity measurements within the region-of-interest (ROI) were normalized to values at 2 h post-injection as this timepoint gave rise to the highest intensities in a consistent manner. This proved to be a critical step in our analysis, as the predicted half-lives depended greatly on a monotonic decay from this 2 h timepoint. Using this approach, we measured the decay half-life of the SF-Cy7 protein in solution to be 12.6 h (± 2.2 h) in the rat knee, which corresponds with the intra-articular clearance of macromolecules, such as hyaluronan and albumin, when studied using radiographic scintigraphy and other accepted synovial fluid and blood sampling techniques (Betre et al. 2006, Christensen et al. 1982, Page-Thomas et al. 1987, Simkin and Benedict 1990). In small-animal models of intra-articular clearance, small molecules of less than 5 kDa in size are cleared within minutes to an hour, while larger molecules (varying from 5 kDa to 50 kDa) persist in the joint space longer, with half-lives between 1–6 h. Thus, the use of fluorescent, *in vivo* imaging with ROI normalization as described has provided a similar measure of the intra-articular clearance of large macromolecules (>50 kDa), with decay values falling within the expected range of 6–25 h (Denlinger, Page-Thomas et al. 1987, Rodnan and Maclachlan 1960, Simkin and Benedict 1990). We determined that the SF-Cy7 microparticle drug delivery system contributed to an increased Cy7 residence time based on the decay half-life of 43.3 h (±14.4 h). Overall, the higher clearance rates for the SF microparticles in the joint space, as compared to the comparatively slow in vitro release rates, give evidence of a role for lymphatic clearance in driving joint residence of injected solutes. At this rate of clearance, if only nanograms of drug are needed to have a pharmacological effect on the joint tissue, the SF microparticles could sustain the retention of such quantities for approximately twenty six days when as little as 100 μg of drug is utilized (100 mg of SF particles contains 240 μg of Cy7).

Fluorescent in-vivo imaging was also used to reveal differences between SF-Cy7 microparticles and SF-Cy7 protein solution injections in the radial distribution of the fluorescence within each joint. Microparticle-injected limbs exhibited bright fluorescence signal concentrated within the joint and fluorescence values declined steeply away from the joint. SF-Cy7 protein solution-injected joints were more diffuse in fluorescence, and fluorescence values declined more gradually away from the joint cavity. By determining a RD_{50} term, the distance at which the normalized fluorescence fell to 50% of maximum, statistical comparisons between groups could be made at different time points. This analysis revealed that higher fluorescence values, corresponding to higher levels of Cy7 dye, accumulate in extra-articular tissues for SF-Cy7 solution-injected joints, nearly approaching significant differences between Time 0 and 24 h (RD_{50} = 0.56 mm and 1.0 mm respectively; $p = 0.11$). The radial distribution of fluorescence for SF-Cy7 microparticles remains approximately constant between Time 0 and 24 h post-injection (RD_{50} = 0.17 and 0.20 mm, respectively). This suggests that SF microparticles can reduce extra-articular exposure to

injected small-molecules by localizing them to the joint cavity and that fluorescence, *in vivo* imaging can be used to compare the biodistribution of intra-articular injections.

While currently no intra-articular drug delivery system has been shown to yield sustained release of drug locally for months, some strategies have still been able to realize efficacy in animal models of OA. Betre and co-workers utilized an elastin-like polypeptide (ELP) system to deliver a protein drug (IL1-Ra) and achieve a joint half-life of 3.7 days, by scintigraphic measurement (Betre et al. 2006). As Allen and colleagues showed, this drug delivery system proved more efficacious than a single injection of IL-1Ra alone within the first 6 days post-treatment, by histological and symptomatic measures, in a rat IL-1β over-expression model of OA (Allen and Cott 2010, Allen et al. 2011). Similarly, Thakkar and co-workers applied chitosan microspheres to deliver the small-molecule drug, celecoxib, by intra-articular injection in a rat model of adjuvant-induced OA. Though *in vitro* studies revealed that the full load of drug was released within the first 96 h, the extended release of the chitosan microspheres had a significant effect on the reduction on OA lesions *in vivo* when compared to the saline control and celecoxib suspension at 18 d post-injection (Thakkar et al. 2004). Such studies highlight the potential of our silk microparticle system, paired with a potent drug, to have disease-modifying efficacy over multiple weeks or months.

Conclusion

SF microparticle drug carriers can be used to overcome the shortcomings of the intra-articular delivery of small-molecule drugs for the treatment of OA. The formed SF particles are of micron dimensions sufficient to increase joint residence time and limit rapid clearance of loaded drug. Live-animal fluorescence imaging is a useful tool for measuring the radial biodistribution and joint clearance properties of a drug delivery system when ROI image analysis is employed. Utilizing this tool for analyzing SF microparticle dye retention *in vivo*, we determined the SF microparticles can provide localized and sustained release of loaded small-molecule drugs over several weeks. This study has significant implications on the study of intra-articular drug delivery research and arthritis treatment with small-molecule drugs.

Acknowledgments

This work was supported by the NIH (P01AR050245, P41EB002520, T32GM008555, F31AR063610-01 and F32AR063012).

List of Abbreviations

SF	Silk fibroin
SF-Cy	Cy7-bound silk fibroin protein
OA	Osteoarthritis
NSAIDs	Non-steroidal anti-inflammatory drugs
PLGA	Poly-(lactide-co-glycolide) acid

ELPs	Elastin-like polypeptides
SEM	Scanning electron microscopy
SF-Cy7100%	Un-mixed SF-Cy7
SF-Cy750%	A 1:1 mixture of SF-Cy7 and SF solutions
SF-Cy733%	A 1:2 mixture of SF-Cy7 and SF solutions
PVA	Poly-vinyl alcohol
MeOH	Methanol
IACUC	Institutional Animal Care and Use Committee
IVIS	In-vivo imaging system
ROI	Region of interest
T-NF	Total normalized fluorescence
RD-50	Radial distance at which normalized fluorecence equals 50% of maximum
ANOVA	Analysis of variance
IL-1Ra	Interleukin-1 receptor antagonist

References

Adams SB Jr, Shamji MF, Nettles DL, Hwang P, Setton LA. Sustained release of antibiotics from injectable and thermally responsive polypeptide depots. J Biomed Mater Res B Appl Biomater. 2009; 90(1):67–74. [PubMed: 18988275]

Allen DD, Cott CA. Evaluating rehabilitation outcomes from the client's perspective by identifying the gap between current and preferred movement ability. Disabil Rehabil. 2010; 32(6):452–461. [PubMed: 19852715]

Allen KD, Adams SB Jr, Mata BA, Shamji MF, Gouze E, Jing L, Nettles DL, Latt LD, Setton LA. Gait and behavior in an IL1beta-mediated model of rat knee arthritis and effects of an IL1 antagonist. J Orthop Res. 2011; 29(5):694–703. [PubMed: 21437948]

Altman GH, Diaz F, Jakuba C, Calabro T, Horan RL, Chen J, Lu H, Richmond J, Kaplan DL. Silk-based biomaterials. Biomaterials. 2003; 24(3):401–416. [PubMed: 12423595]

Arai TF, Innocenti G, Tsukada RM. Biodegradation of B. mori silk fibroin fibers and films. J Appl Polym Sci. 2004; 91:2383–2390.

Ayral X. Injections in the treatment of osteoarthritis. 2001; 15(4)

Betre H, Liu W, Zalutsky MR, Chilkoti A, Kraus VB, Setton LA. A thermally responsive biopolymer for intra-articular drug delivery. J Control Release. 2006; 115(2):175–182. [PubMed: 16959360]

Bitton R. The Economic Burden of Osteoarthritis. American Journal of Managed Care. 2009:S230–235. [PubMed: 19817509]

Bowles RD, Mata BA, Bell RD, Mwangi TK, Huebner JL, Kraus VB, Setton LA. In Vivo luminescent imaging of NF-kappaB activity and serum cytokine levels predict pain sensitivities in a rodent model of osteoarthritis. Arthritis Rheum. 2013

Butoescu N, Jordan O, Burdet P, Stadelmann P, Petri-Fink A, Hofmann H, Doelker E. Dexamethasone-containing biodegradable superparamagnetic microparticles for intra-articular administration: physicochemical and magnetic properties, in vitro and in vivo drug release. Eur J Pharm Biopharm. 2009; 72(3):529–538. [PubMed: 19303928]

Butoescu N, Jordan O, Doelker E. Intra-articular drug delivery systems for the treatment of rheumatic diseases: a review of the factors influencing their performance. Eur J Pharm Biopharm. 2009; 73(2):205–218. [PubMed: 19545624]

Cao Y, Wang B. Biodegradation of Silk Biomaterials. 2009; 10(4):1514–1524.

Cao Y, Wang B. Biodegradation of silk biomaterials. Int J Mol Sci. 2009; 10(4):1514–1524. [PubMed: 19468322]

Christensen SB, Reimann I, Henriksen O, Arnoldi CC. Experimental osteoarthritis in the rabbit. A study of 133 xenon washout rates from the synovial cavity. Acta Orthop Scand. 1982; 53(2):167–174. [PubMed: 7136561]

Denlinger, JL. Metabolism of sodium hyaluronate in articular and ocular tissues.

Evans CH, Kraus VB, Setton LA. Progress in intra-articular therapy. Nat Rev Rheumatol. 2014; 10(1): 11–22. [PubMed: 24189839]

Gerwin N, Hops C, Lucke A. Intraarticular drug delivery in osteoarthritis. Adv Drug Deliv Rev. 2006; 58(2):226–242. [PubMed: 16574267]

Gobin AS, Rhea R, Newman RA, Mathur AB. Silk-fibroin-coated liposomes for long-term and targeted drug delivery. Int J Nanomedicine. 2006; 1(1):81–87. [PubMed: 17722265]

Hofmann S, Foo CT, Rossetti F, Textor M, Vunjak-Novakovic G, Kaplan DL, Merkle HP, Meinel L. Silk fibroin as an organic polymer for controlled drug delivery. J Control Release. 2006; 111(1–2): 219–227. [PubMed: 16458987]

Horan RL, Antle K, Collette AL, Wang Y, Huang J, Moreau JE, Volloch V, Kaplan DL, Altman GH. In vitro degradation of silk fibroin. Biomaterials. 2005; 26(17):3385–3393. [PubMed: 15621227]

Horisawa E, Hirota T, Kawazoe S, Yamada J, Yamamoto H, Takeuchi H, Kawashima Y. Prolonged anti-inflammatory action of DL-lactide/glycolide copolymer nanospheres containing betamethasone sodium phosphate for an intra-articular delivery system in antigen-induced arthritic rabbit. Pharm Res. 2002; 19(4):403–410. [PubMed: 12033371]

Horisawa E, Kubota K, Tuboi I, Sato K, Yamamoto H, Takeuchi H, Kawashima Y. Size-dependency of DL-lactide/glycolide copolymer particulates for intra-articular delivery system on phagocytosis in rat synovium. Pharm Res. 2002; 19(2):132–139. [PubMed: 11883639]

Hough, A, Jr. A Textbook of Rheumatology. Philadelphia: Lippincott Williams & Wilkins; 2005. Pathology of osteoarthritis. Arthritis and Allied Conditions.

Jones, A.; Doherty, M. Osteoarthritis. New York: Oxford University Press; 2003. Intra-articular glucocorticoids and other injection therapies.

Kang ML, Im GI. Drug delivery systems for intra-articular treatment of osteoarthritis. Expert Opin Drug Deliv. 2014; 11(2):269–282. [PubMed: 24308404]

Kim UJ, Park J, Kim HJ, Wada M, Kaplan DL. Three-dimensional aqueous-derived biomaterial scaffolds from silk fibroin. Biomaterials. 2005; 26(15):2775–2785. [PubMed: 15585282]

Kumar AB, Blanks AM, Bodick RCN. Sustained Efficacy of Intra-articular FX006 In a Rat Model of Osteoarthritis. Osteoarthritis and Cartilage. 2013; 20:S289. April 2012.

Lammel AS, Hu X, Park SH, Kaplan DL, Scheibel TR. Controlling silk fibroin particle features for drug delivery. Biomaterials. 2010; 31(16):4583–4591. [PubMed: 20219241]

Liang LS, Jackson J, Min W, Risovic V, Wasan KM, Burt HM. Methotrexate loaded poly (L-lactic acid) microspheres for intra-articular delivery of methotrexate to the joint. J Pharm Sci. 2004; 93(4):943–956. [PubMed: 14999731]

Liggins RT, Cruz T, Min W, Liang L, Hunter WL, Burt HM. Intra-articular treatment of arthritis with microsphere formulations of paclitaxel: biocompatibility and efficacy determinations in rabbits. Inflamm Res. 2004; 53(8):363–372. [PubMed: 15316667]

Lopez-Garcia F, Vazquez-Auton JM, Gil F, Latoore R, Moreno F, Villalain J, Gomez-Fernandez JC. Intra-articular therapy of experimental arthritis with a derivative of triamcinolone acetonide incorporated in liposomes. J Pharm Pharmacol. 1993; 45(6):576–578. [PubMed: 8103110]

Lu Q, Zhang B, Li M, Zuo B, Kaplan DL, Huang Y, Zhu H. Degradation mechanism and control of silk fibroin. Biomacromolecules. 2011; 12(4):1080–1086. [PubMed: 21361368]

Meinel L, Hofmann S, Karageorgiou V, Kirker-Head C, McCool J, Gronowicz G, Zichner L, Langer R, Vunjak-Novakovic G, Kaplan DL. The inflammatory responses to silk films in vitro and in vivo. Biomaterials. 2005; 26(2):147–155. [PubMed: 15207461]

Meinel L, Kaplan DL. Silk constructs for delivery of musculoskeletal therapeutics. Adv Drug Deliv Rev. 2012; 64(12):1111–1122. [PubMed: 22522139]

Numata K, Kaplan DL. Silk-based delivery systems of bioactive molecules. Adv Drug Deliv Rev. 2010; 62(15):1497–1508. [PubMed: 20298729]

Owen SG, Francis HW, Roberts MS. Disappearance kinetics of solutes from synovial fluid after intra-articular injection. 1994; 38(4)

Page-Thomas DP, Bard D, King B, Dingle JT. Clearance of proteoglycan from joint cavities. Ann Rheum Dis. 1987; 46(12):934–937. [PubMed: 3426302]

Poole, AR.; Howell, DS. Diagnosis and Medical/Surgical Management. Philadelphia: W.B. Saunders Company; 2001. Etiopathogenesis of Osteoarthritis. Osteoarthritis.

Ratcliffe JH, Hunneyball IM, Wilson CG, Smith A, Davis SS. Albumin microspheres for intra-articular drug delivery: investigation of their retention in normal and arthritic knee joints of rabbits. J Pharm Pharmacol. 1987; 39(4):290–295. [PubMed: 2884293]

Rockwood DN, Preda RC, Yucel T, Wang X, Lovett ML, Kaplan DL. Materials fabrication from Bombyx mori silk fibroin. Nat Protoc. 2011; 6(10):1612–1631. [PubMed: 21959241]

Rodnan GP, Maclachlan MJ. The absorption of serum albumin and gamma globulin from the knee joint of man and rabbit. Arthritis & Rheumatism. 1960; 3(2):152–157. [PubMed: 14438185]

Simkin PA, Benedict RS. Iodide and albumin kinetics in normal canine wrists and knees. Arthritis Rheum. 1990; 33(1):73–79. [PubMed: 2302270]

Srihanam P, Simcheur W, Srisuwan Y. Study on silk sericin and chitosan blend film: morphology and secondary structure characterizations. Pak J Biol Sci. 2009; 12(22):1487–1490. [PubMed: 20180324]

Thakkar H, Sharma RK, Mishra AK, Chuttani K, Murthy RS. Celecoxib incorporated chitosan microspheres: in vitro and in vivo evaluation. J Drug Target. 2004; 12(9–10):549–557. [PubMed: 15621680]

Turker S, Erdogan S, Ozer AY, Ergun EL, Tuncel M, Bilgili H, Deveci S. Scintigraphic imaging of radiolabelled drug delivery systems in rabbits with arthritis. Int J Pharm. 2005; 296(1–2):34–43. [PubMed: 15885453]

Vepari C, Kaplan DL. Silk as a Biomaterial. 2007; 32(8–9):991–1007.

Wallis WJ, Simkin PA, Nelp WB, Foster DM. Intraarticular volume and clearance in human synovial effusions. Arthritis Rheum. 1985; 28(4):441–449. [PubMed: 3885961]

Wang X, Yucel T, Lu Q, Hu X, Kaplan DL. Silk nanospheres and microspheres from silk/pva blend films for drug delivery. Biomaterials. 2010; 31(6):1025–1035. [PubMed: 19945157]

Whitmire RE, Wilson DS, Singh A, Levenston ME, Murthy N, Garcia AJ. Self-assembling nanoparticles for intra-articular delivery of anti-inflammatory proteins. Biomaterials. 2012; 33(30):7665–7675. [PubMed: 22818981]

Wigginton SM, Chu BC, Weisman MH, Howell SB. Methotrexate pharmacokinetics after intrarticular injection in patients with rheumatoid arthritis. Arthritis & Rheumatism. 1980; 23(1):119–122. [PubMed: 6965451]

Zhang W, Moskowitz RW, Nuki G, Abramson S, Altman RD, Arden N, Bierma-Zeinstra S, Brandt KD, Croft P, Doherty M, Dougados M, Hochberg M, Hunter DJ, Kwoh K, Lohmander LS, Tugwell P. OARSI recommendations for the management of hip and knee osteoarthritis, Part II: OARSI evidence-based, expert consensus guidelines. Osteoarthritis Cartilage. 2008; 16(2):137–162. [PubMed: 18279766]

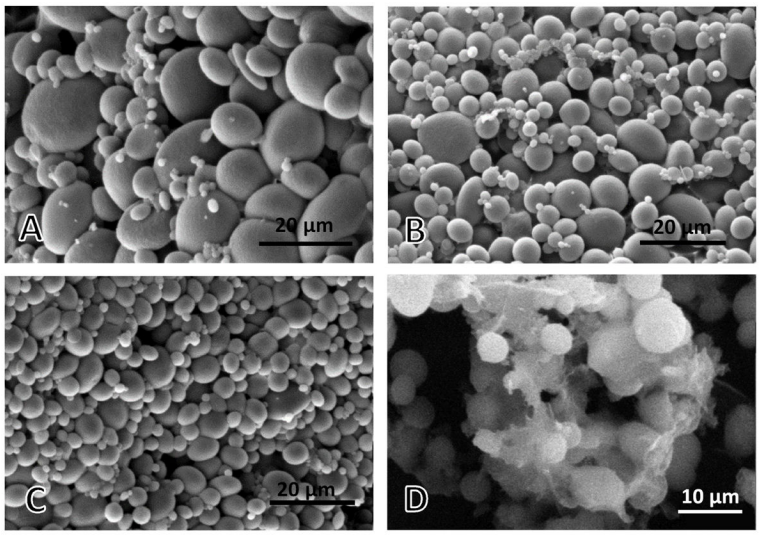

Figure 1.

Scanning electron microscopic images of silk fibroin-Cy7 particles fabricated using (**A**) silk fibroin-Cy7 solution only (SF-Cy7$_{100\%}$), (**B**) silk fibroin-Cy7 solution mixed with unlabeled silk fibroin at 1:1 ratio (SF-Cy7$_{50\%}$), (**C**) silk fibroin-Cy7 solution mixed with unlabeled silk fibroin at 1:2 ratio (SF-Cy7$_{33\%}$), (**D**) SF-Cy7$_{33\%}$ particles after SF coating process.

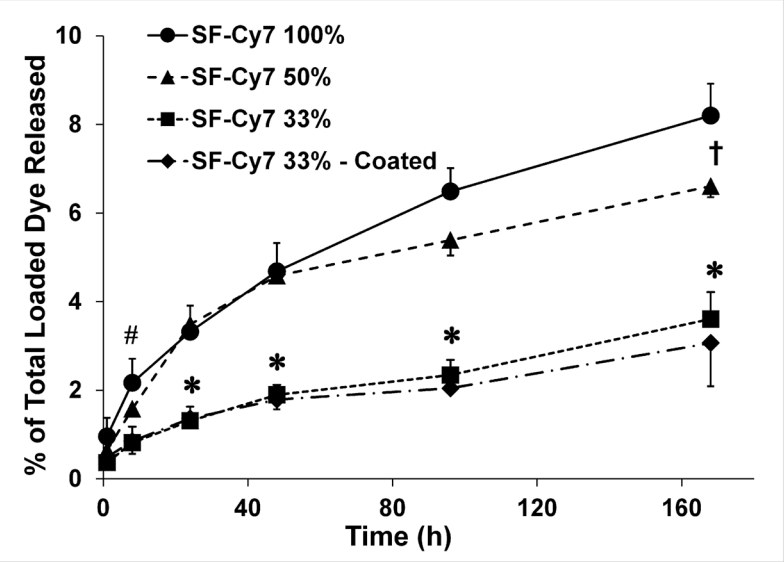

Figure 2.

In vitro cumulative release of Cy7 drug from different silk fibroin-Cy7 (SF-Cy7) microparticle formulations. A two-factor analysis of variance was used to determine statistical differences between formulations at each time point. * = $p<0.05$ for SF-$Cy7_{33\%}$ vs. SF-$Cy7_{100\%}$ and SF-$Cy7_{50\%}$; # = $p<0.05$: SF-$Cy7_{33\%}$ vs. SF-$Cy7_{100\%}$; †=$p<0.05$: SF-$Cy7_{50\%}$ vs. SF-$Cy7_{100\%}$.

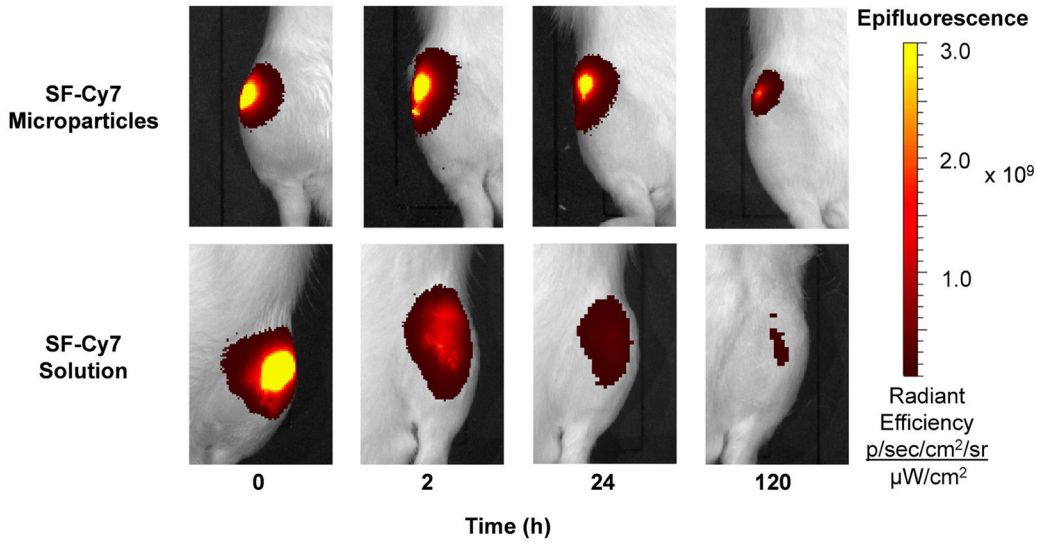

Figure 3.

In vivo imaging of intra-articular injections of SF-Cy7 particles or SF-Cy7 solution in rat knee joints over 5 days. Representative images of microparticle-injected knees display a more focused and persistent fluorescence intensity than in protein solution-injected knees.

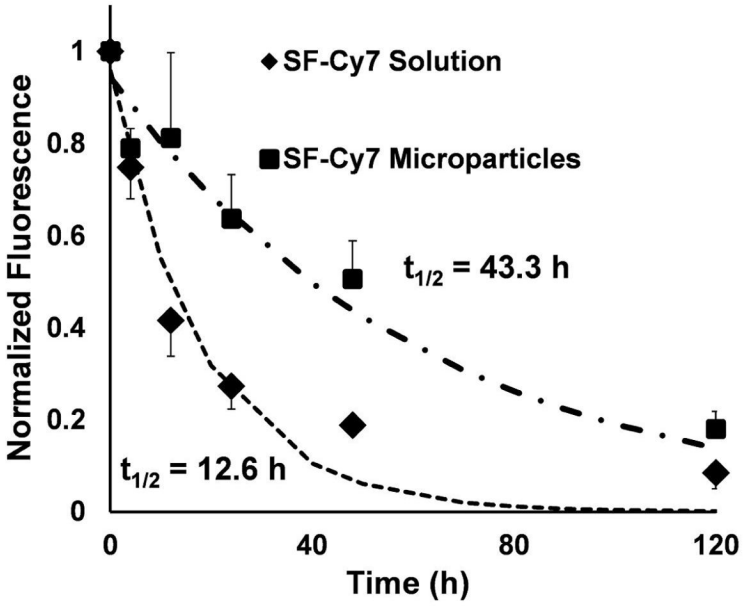

Figure 4.

Mean ROI fluorescence measured longitudinally over 5 days in the rat knee joints normalized to ROI fluorescence at 2 h post-injection. Normalized fluorescence curves for each injection group were curve-fit for mono-exponential decay to determine a decay half-life ($t_{1/2}$). Unpaired t-test analysis revealed that $t_{1/2}$ are statistically different between SF-Cy7 microparticles and SF-Cy7 solution (43.3 h, ±14.4 h and 12.6 h, ±2.2 h, respectively; $p<0.05$).

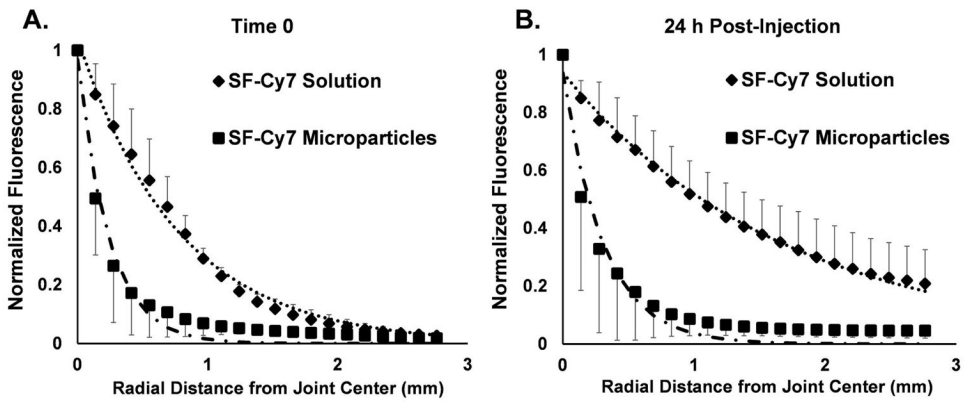

Figure 5.

Mean normalized fluorescence was assessed radially from the center of the joint and fit to a mono-exponential decay equation. (**A**) The radial distribution of fluorescence at Time 0 falls rapidly for microparticle-injected joints (RD_{50}= 0.17 mm) and less rapidly for SF-Cy7 solution group at Time 0 (RD_{50}= 0.56 mm, $p<0.01$ vs. microparticle injection). (**B**) The radial distribution of fluorescence at 24 h post-injection continues to decline steeply for microparticle-injected joints (RD_{50}= 0.20 mm) but the distribution becomes even more disperse for SF-Cy7 solution-injected joints (RD_{50} = 1.0 mm, $p<0.05$ vs. microparticle injection).

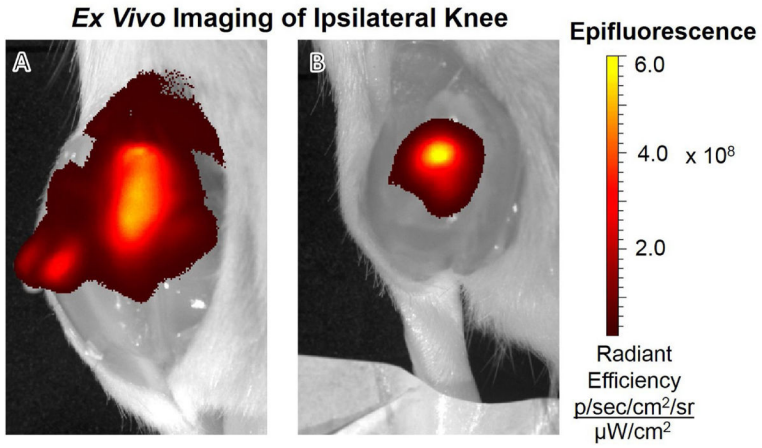

Figure 6.

Ex vivo imaging of rat ipsilateral knee after exposure of the intra-articular cavity post-sacrifice on day 5. (**A**) Fluorescence intensity of SF-Cy7 solution treated joint is lower in peak values and more distributed to neighboring joint tissues. (**B**) Fluorescent intensity ofSF-Cy7 microparticle-injected joint is more confined to the intra-articular cavity, with higher peak values in the joint and reduced distribution to neighboring tissue.

Table I

SF microparticle size distribution for each formulation based on scanning electron microscopy image analysis.

Formulation	Diameter (μm) (Mean + SD)	Range (μm)
SF-Cy7$_{100\%}$	7.4 ± 2.1	0.746 – 21.6
SF-Cy7$_{50\%}$	5.3 ± 3.0	0.598 – 14.9
SF-Cy7$_{33\%}$	3.8 ± 1.9	1.0 – 9.8